IEEE Access
Multidisciplinary ⋮ Rapid Review ⋮ Open Access Journal

Received October 4, 2021, accepted October 17, 2021, date of publication October 19, 2021, date of current version October 26, 2021.

Digital Object Identifier 10.1109/ACCESS.2021.3121399

Generalized Regression Neural Network Based Fast Fading Channel Tracking Using Frequency-Domain CSI Smoothing

SHUN KOJIMA[1], (Member, IEEE), HE HE[2], (Graduate Student Member, IEEE), TAKAKI OMURA[3], KAZUKI MARUTA[4], (Senior Member, IEEE), AND CHANG-JUN AHN[2], (Senior Member, IEEE)

[1]Graduate School of Engineering, Utsunomiya University, Tochigi 321-8585, Japan
[2]Graduate School of Engineering, Chiba University, Chiba 263-8522, Japan
[3]SoftBank Corporation, Tokyo 105-0022, Japan
[4]Academy for Super Smart Society, Tokyo Institute of Technology, Tokyo 152-8552, Japan

Corresponding author: Shun Kojima (s.kojima@ieee.org)

This work was supported in part by the Artificial Intelligence Research Promotion Foundation, and in part by the KAKENHI Grant-in-Aid for Scientific Research (B) under Grant 20H04178.

ABSTRACT In the high mobility environment, the channel state information (CSI) in the last part of the packet is different from the beginning part's actual channel. This phenomenon degrades channel estimation accuracy, and hence it is necessary to be compensated to realize reliable communications. Decision feedback channel estimation (DFCE) has been widely considered as the channel tracking approach. It still causes estimation errors due to the decision-making process in the presence of time and frequency selective fading environments. To address these issues, this paper newly proposes a generalized regression neural network (GRNN) based channel tracking scheme incorporated with frequency-domain CSI smoothing. The latter part is the key to improve the dependability of the training data sets. Computer simulation results confirm that the proposed scheme can achieve superior BER performance and the lower root mean square error (RMSE) value of estimated CSI better than the conventional ones.

INDEX TERMS OFDM, fast fading, channel estimation, neural network, GRNN, smoothing, Savitzky-Golay filtering.

I. INTRODUCTION

Packet-based transmission has been the most common wireless communication method, in which the desired transmission bitstream is divided into packets and transmitted. In this case, the propagation channel needs to be estimated for each packet in order to accurately equalize and decode the signal. The pilot-aided channel estimation (PCE) is one of the basic methods for channel estimation. In PCE, known training symbols are generally inserted at the head of the packet. In a static environment, it can estimate the frequency selectivity of channel state information (CSI). However, there is a growing demand for reliable and high-capacity communications even in an environment where transmitters and receivers move at high speed. Under such a fast moving environment, the channel state rapidly changes in the time-domain. Accordingly, estimated CSI by PCE is largely dissimilar to the actual channel state, particularly in the last part of the packet.

Many challenges have been made so far to trace the channel state transition [1]–[5]. In [1], a data-aided decision feedback channel estimation (DFCE) was proposed. DFCE directly estimates channel variation at any specific data symbol using the difference between the received symbol and the replica signal which is the multiplication of remodulated signal by CSI obtained by PCE. The authors in [2] proposed a computationally efficient channel estimation for an OFDM system with space-time coding in time-varying dispersive multipath fading channels. In [3], the low-complexity windowed DFT-based minimum mean square error (MMSE) channel estimator was proposed. These methods reduced the computation complexity without degrading the channel estimation performance. In [4], the authors proposed the pilot-based channel estimation scheme on a rapidly-varying

The associate editor coordinating the review of this manuscript and approving it for publication was Junhua Li.

channel environment in OFDM systems. It used channel interpolation to handle rapid variation within a transmission block. Moreover, subspace-based channel estimation techniques for OFDM systems over fast-fading channels have been proposed [5]. Although these precedent channel estimation approaches are tolerant of fast fading environments, their computation complexity have not been evaluated.

The recent advancement of machine learning technologies has enabled its application to a variety of fields. In wireless communications, several applications are being actively investigated. Automatic modulation recognition is the most widely known application of machine learning to signal processing technology [6], [7]. Emerging approaches have been proposed to estimate communication environment, mainly for SNR [8], K-factor [9], and Doppler shift estimation [10]. There are also many methods for channel estimation using machine learning [11]–[13]. Literature in [11] proposed the data-aided MIMO channel estimation using the support vector machine (SVM) based on regression of multiple variables. This method shows better estimation accuracy in nonlinear channels. In [12], the authors proposed to employ deep neural networks for channel estimation and symbol detection in an OFDM system. The model is trained offline using simulation data where the wireless channel was considered as black boxes. The simulation results indicated that the deep learning method is beneficial when the wireless channel is complicated by severe distortions and interference. Authors in [13] proposed deep learning-based super-resolution channel and direction of arrival (DOA) estimation in massive MIMO systems. While machine learning is an effective method for channel estimation, there are still issues in considering its effectiveness in high-speed mobile environments.

In view of the above background, we previously proposed a multilayer feedforward neural network (MLFNN) based channel tracking scheme which is effective even in fast-moving environments [14]. It employs MLFNN to estimate the whole channel state transition and compensates the channel variation using the generalization capability derived from the relationship between inputs and outputs. MLFNN is trained by partially obtained CSI by DFCE in the beginning part of the packet. It showed satisfactory tracking performance against channel variations. Meanwhile, there was a need for improvement in terms of estimation accuracy and computational complexity. We then conceived its extension by using a generalized regression neural network (GRNN) [15]. A one-pass learning process of GRNN can eliminate the iterative training process without impairing the generalization capability. While these methods show superior performance in fast-moving environments, these channel tracking performance depend on the accuracy of CSI used for the supervised data. Especially, DFCE sometimes produces incorrect CSI due to decision errors when the channel state transition has a sharp fluctuation even in the beginning part of the packet. For that reason, estimator has to reduce the difference between data-aided CSI and real channel state to achieve further improvement of BER performance.

In order to overcome this problem, this paper newly proposes a frequency-domain CSI smoothing scheme for GRNN based channel tracking method. Smoothed CSI can compensate the inaccuracy of data for supervised training and it can improve the BER performance. Our proposal applies Savitzky-Golay (SG) filtering which can provide outstanding smoothing capability of data-aided CSI and thus it can contribute to more precise GRNN training. In many cases, the values of CSIs in neighboring subcarriers are similar; behave as if it had continuity. If DFCE produces inaccurate CSI in some subcarriers, the estimated frequency selectivity is dispersed in various places. SG smoothing method can eliminate or mitigate such influence of dispersed data in consideration with the importance of not only specific but also peripheral information. Accordingly, the frequency selectivity of data-aided CSI becomes more accurate than the conventional method by dispersed data correction capability of SG smoothing method. Finally, the estimated whole channel state transition by GRNN can be more accurate in time domain after the smoothing process. To summarize, key contributions of this paper are:

1) To rectify the impact of inaccurate CSI and estimate the whole channel state transition accurately even if data-aided CSI is in error.
2) To achieve high-precision channel estimation with limited CSI information even under a high-speed mobile environment.

The rest of this paper is structured as follows. Section II defines the channel model and OFDM system. Section III describes the conventional approach. Section IV describe smoothing methods and present the proposed approach concretely. The simulation results are disclosed in Section V. Finally, Section VI concludes the paper.

II. SYSTEM MODEL

A. CHANNEL MODEL

We assume Jakes' time-varying multipath fading channel as the channel model of the wireless communications system. It is composed of L discrete paths with different time delays. Its impulse response is expressed as,

$$h(\tau, t) = \sum_{l=0}^{L-1} h_l(t)\delta(\tau - \tau_l), \tag{1}$$

$$h_l(t) = \frac{g_l}{\sqrt{Q}} \sum_{q=1}^{Q} exp\left[j\left(\omega_D t\ cos\alpha_q + \phi_q\right)\right], \tag{2}$$

where h_l and τ_l denote the complex channel coefficient and the time delay of the l-th propagation path, respectively. g_l, α_q and ϕ_q are the l-th path gain, angle of arrival of the q-th wave and its initial phase, respectively. ω_D represents the maximum Doppler radian frequency shift, i.e. $\omega_D = 2\pi f_D$, where f_D presents the maximum Doppler frequency. Here assumes normalized path gain, i.e. $\sum_{p=0}^{L-1} E\left[|h_l|^2\right] = 1$, where $E[\cdot]$ indicates the ensemble average (expectation) operation. It is well-known that the probability density function

of $|h_l|$ has Rayleigh distribution in non-line-of-sight communication. The multipath fading which has this feature is called Rayleigh fading. From Eq. (2), we can confirm that the channel coefficient has the time-varying component and high-speed mobile environment makes the variation more drastically. The frequency response $H(f, t)$ via Fourier transform of the impulse response can be obtained as,

$$\begin{aligned} H(f, t) &= \int_0^{\infty} h(\tau, t) exp(-j2\pi f \tau) d\tau \\ &= \sum_{l=0}^{L-1} h_l(t) exp(-j2\pi f \tau_l), \end{aligned} \tag{3}$$

where f denotes the frequency component. The frequency response is generally not flat in a mobile communication environment. Frequency selective fading channel is provided by $L > 1$ where the discreet expression of $|H(f, t)|$ fluctuates. Because of this fading, the received signal level and phase component significantly vary in the transmission frequency bandwidth as in Fig. 1, especially in case of broadband transmission [16], [17].

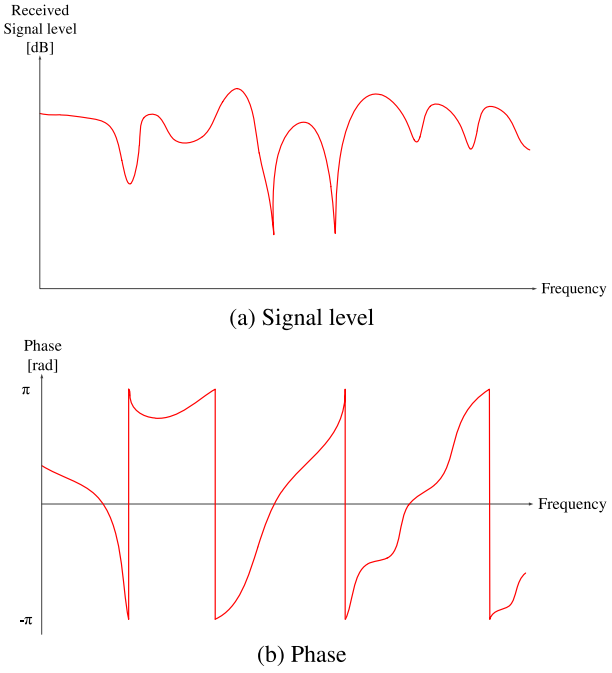

(a) Signal level

(b) Phase

FIGURE 1. Frequency selective fading channel.

From these equations, it can be observed that the multipath fading channel varies with the Doppler shift, which is proportional to the transceiver's velocity of movement. Therefore, general channel estimation is greatly affected by the Doppler shift, causing degradation in decoding performance and throughput, especially in fast-moving environments. The objective of this paper is to compensate for these influences and to improve the BER performance.

B. OFDM SYSTEM

Orthogonal Frequency Division Multiplexing (OFDM) is adopted for many commercial wireless standards which include IEEE 802.11 wireless local area networks, IEEE 802.16 wireless metropolitan area networks, and 3GPP long term evolution cellular networks [18]. The system uses subcarriers which are orthogonal to each other. OFDM system converts a high-speed transmission signal into a low-speed and narrow-band signal for a parallel transmission on a frequency characteristic. OFDM can improve the utilization efficiency of a frequency band. In addition, each subcarrier can make the length of signal longer. This can prevent inter-symbol interferences by using a guard interval. From these advantages, OFDM system is suitable for mobile communication. Fig. 2 shows the original system model of OFDM transmitter and receiver.

III. CONVENTIONAL NN BASED CHANNEL TRACKING

A. DECISION FEEDBACK CHANNEL ESTIMATION (DFCE)

Here we assume that single-input single-output based orthogonal frequency division multiplexing (SISO-OFDM) transmission and the insertion of a pilot symbol at the beginning of the packet. The DFCE can estimate the CSI of a particular data symbol using the demodulated signal and the CSI obtained by the PCE. Fig. 3 shows the process of DFCE for the i-th data symbol and the characteristic of time-varying channel. The received signal of the m-th subcarrier and the n-th data symbol, $Y(m, n)$, is represented as follows:

$$Y(m, n) = H(m, n)X(m, n) + N(m, n), \tag{4}$$

where $H(m, n)$, $X(m, n)$, and $N(m, n)$ indicate the channel coefficient, the transmitted symbol, and Additive white Gaussian noise (AWGN), respectively [19]. Given the pilot symbol $X(m)$, CSI $\tilde{H}(m)$ is estimated as

$$\begin{aligned} \tilde{H}(m) &= \frac{Y(m)}{X(m)} \\ &= H(m, n) + \frac{N(m, n)}{X(m, n)}. \end{aligned} \tag{5}$$

It is used for subcarrier equalization and the decision result of the n-th transmitted data symbol is then obtained.

$$\hat{X}(m, n) = \mathcal{F}\left[\frac{Y(m, n)}{\tilde{H}(m)}\right], \tag{6}$$

where $\mathcal{F}(m)[.]$ stands for the decision function. Dada-aided CSI at the n-th symbol $\check{H}(m, n)$ can be derived as,

$$\begin{aligned} \check{H}(m, n) &= \frac{Y(m, n)}{\hat{X}(m, n)} \\ &= H(m, n)\frac{X(m, n)}{\hat{X}(m, n)} + \frac{N(m, n)}{\hat{X}(m, n)}. \end{aligned} \tag{7}$$

At this point, CSI is contaminated due to the additive noise effect and decision failure in (6), which may cause degradation of demodulation accuracy. The noise reduction is possible by using adjacent symbols. Here CSI is averaged

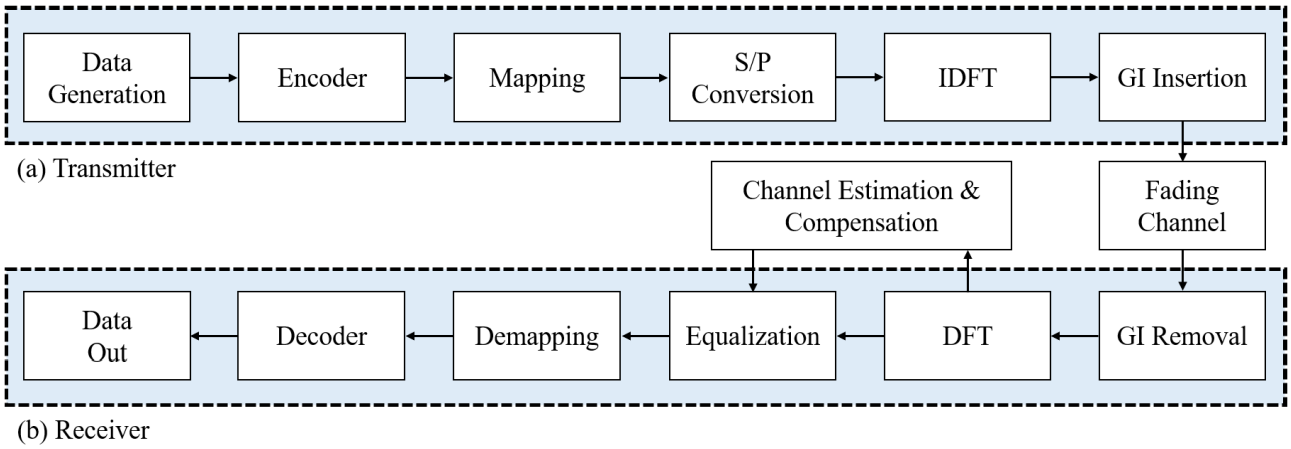

FIGURE 2. The block diagram of the proposed OFDM transmitter and receiver.

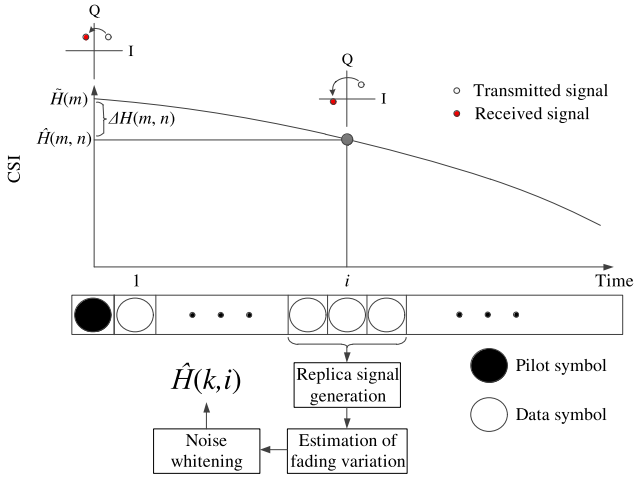

FIGURE 3. The process of decision feedback channel estimation and the characteristic of a channel variation.

over adjacent three samples [20]: $\check{H}(m, n-1)$, $\check{H}(m, n)$ and $\check{H}(m, n+1)$,

$$\hat{H}(m, n) = \frac{\sum_{i=n-1}^{n+1} \check{H}(m, i)}{3}. \tag{8}$$

For the purpose of tracking the whole channel state transition, DFCE based channel estimation is performed for all symbol instants [21], [22]. However, this method sometimes estimates inaccurate CSI due to decision errors. Thus, the channel tracking performance cannot be increased even though CSI given DFCE is applied under the fast fading environment. Specifically, decision errors have often happened in the last part of the packet. This is because the channel variation from the pilot-aided CSI to the channel state is quite huge especially at the last part of the packet.

B. NEURAL NETWORK (NN)

Because of the low reliability of DFCE in the last part of the packet, additional approach is needed to stabilize the whole CSI transition using partially obtained CSI at the beginning part of the packet. To resolve this problem, we previously proposed the NN-aided approach [14], [15]. This method applies a NN for channel tracking using partially obtained CSI by PCE and DFCE. The NN can construct relationships between input signals and output signals because of a nonlinear statistical modeling capability [23]. Accordingly, the generalization capability of the NN can achieve high tracing accuracy of whole CSI transition even by training only a few estimated CSI. It is essential to find an optimal structure of hidden layers because of following two perspectives: an unsatisfactory performance produced by few neurons, and the considerable system complexity caused by the oversized hidden layers.

1) MULTILAYER FEEDFORWARD NEURAL NETWORK (MLFNN)

Previous work [14] employed a fully connected 2-layer feed-forward neural network. MLFNN has a layered structure constructed by neurons, and every neuron passes signals to neurons of the next layer. Every MLFNN has an input layer, one or more hidden layers, and an output layer. The input signals of MLFNN are passed directly to the hidden layer in every input neuron. Thus an input layer is not generally counted as layer of MLFNN. The size of input and output layers depend on the size of signals of interest. On the other hand, the system size of hidden layers is variable. One hidden layer normally has sufficient approximation capability to present any continuous function. In general, the sigmoid function is applied for the activation function of hidden layer in regression analysis. The derivative type of this function can be expressed simply using the function itself. Accordingly, using the sigmoid function is suitable for back-propagation (BP) training which is the representative method of the MLFNN training [23]–[25]. However, MLFNN has to renew parameters iteratively in BP training until any training parameter reaches the target value. From this reason, the iterative

process imposes huge computation complexity and causes processing delay.

2) GENERALIZED REGRESSION NEURAL NETWORK (GRNN)

In order to eliminate the iterative training process without impairing the generalization capability, we previously employed GRNN for the NN part [15]. GRNN was originally developed by Donald Specht in 1991 [26]. It is represented as an improved version of the radial basis function neural network (RBFNN), which is based on nonparametric regression. This network can smooth the data transition using sparse training samples using probability distribution from each signal. GRNN sets the weights from the expected value of response directly. Therefore, GRNN does not require any iterative learning process. As shown in Fig. 4, GRNN is constructed by 3 layers except for an input layer: a pattern layer, a summation layer, and an output layer [27].

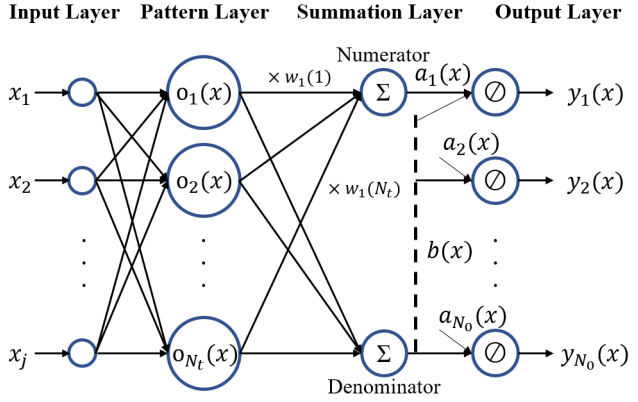

FIGURE 4. Architecture of GRNN.

Following describes how to calculate output values of the 1st output neuron. Let $\mathbf{x} = [x_1, x_2, \ldots, x_j]$ and $\mathbf{c}_i$ denote the input vector and the i-th training input vector ($1 \leq i \leq N_t$), respectively. N_t indicates the number of training sets. The i-th pattern neuron outputs

$$o_i(x) = \exp\left(-\frac{(x - c_i)^2}{r^2}\right), \tag{9}$$

where r denotes the radius of the radial basis function (RBF) applied for the pattern layer. This parameter can adjust the probability distribution and controls a smoothing level of regression results. When r is large, GRNN produces smoother transitions of dispersed training samples and they are not forced to desired outputs. In contrast, small value of r generates rapidly changing regression curves and desired responses are more faithfully tracked by regression results [26]. The output of the i-th pattern neuron is multiplied by the i-th desired response, and inputs to the numerator neuron of the summation layer. Accordingly, the output of the numerator neuron, $a_1(x)$, is calculated by

$$a_1(x) = \sum_{i=1}^{N_t} w_1(i) o_i(x). \tag{10}$$

The output of the denominator neuron, $b(x)$, is generated by

$$b(x) = \sum_{i=1}^{N_t} o_i(x). \tag{11}$$

From (10) and (11), the output at the 1st output neuron, $y_1(x)$, is represented as

$$y_1(x) = b(x)/a_1(x). \tag{12}$$

As mentioned above, GRNN output presents a weighted average of the desired signals when the outputs of the pattern layer are regarded as weights [28], [29]. By replacing $w_1(i)$ with $w_k(i)$ and a_1 with a_k, we can also calculate the output at the k-th output neuron ($k = 1, 2, \ldots, N_o$) using (9)–(12), where N_o denotes the number of GRNN outputs.

C. CONVENTIONAL SCHEME

This paper defines the GRNN-based channel tracking using partially obtained CSI via PCE and DFCE as the conventional scheme [15]. It can obtain accurate estimation results of whole channel state transition thanks to the generalization capability of GRNN trained by estimated CSIs at the beginning and intermediate parts of the packet. It also unnecessitates independent NN training process. Fig. 5 presents the block diagram of the GRNN based channel estimation when the number of subcarriers is N_c. Each output of GRNN ($m = 1, 2, \ldots, N_c - 1, N_c$) corresponds to the m-th subcarrier's CSI. In the GRNN approach, the training inputs and the desired responses are directly applied for the center of each RBF and the multiplication value for the inputs to the numerator neurons of the summation layer, respectively. The GRNN predicts an arbitrary function with the relationship between the input vector and the desired responses by the GRNN training. Before the GRNN training, CSIs are estimated at the 1st data symbol by PCE and the 10th data symbol by DFCE. This information and indices (1, 10) can be set as the desired symbols and training input. By obtaining the CSI by DFCE only in the beginning part of the packet, we can maintain the

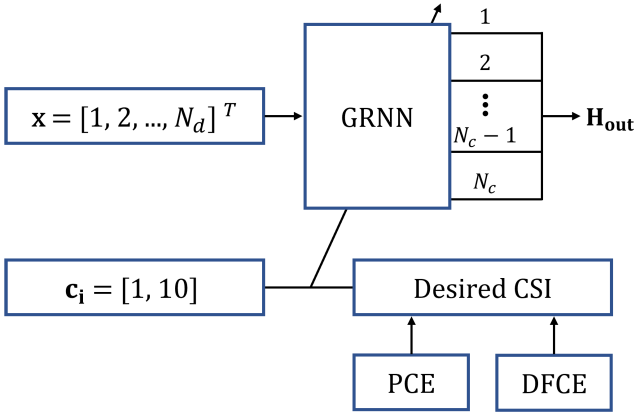

FIGURE 5. Block diagram of the GRNN based channel estimation.

reliability of the desired responses. Each RBF is centered on the pattern layer and multiplication values at nodes from the pattern layer to the numerator neurons are directly defined by the training input and the desired symbols, respectively. Finally, the vector composed of indices for all data symbols $(1, 2, \ldots, N_d)^{\mathsf{T}}$ are entered into the GRNN, where N_d is the number of data symbols. Therefore, GRNN outputs the whole channel state transition represented by

$$\mathbf{H}_{out} = \begin{bmatrix} h_{out}(1,1) & h_{out}(1,2) & \cdots & h_{out}(1,N_d) \\ h_{out}(2,1) & h_{out}(2,2) & \cdots & h_{out}(2,N_d) \\ \vdots & \vdots & \ddots & \vdots \\ h_{out}(N_c,1) & h_{out}(N_c,2) & \cdots & h_{out}(N_c,N_d) \end{bmatrix}, \tag{13}$$

where $h_{out}(m, n)$ $(n = 1, 2, \ldots, N_d)$ is the trained NN based estimated CSI applied for the m-th subcarrier and the n-th data symbol.

Decision errors can happen even in the beginning part of the packet when the channel state transition in the beginning part is quite rapid. Namely, data-aided CSI has some risk of inaccurate information even if DFCE is conducted in the beginning part of the packet. Because of the problem mentioned above, impact of inaccurate CSI caused by the decision error should be alleviated to further improve the performance of channel tracking.

IV. PROPOSAL: FREQUENCY-DOMAIN CSI SMOOTHING

This paper newly proposes to incorporate CSI smoothing method before the GRNN estimation part in the frequency-domain. When DFCE contains some error component, the frequency selectivity of CSI is dispersed; continuity among adjacent subcarriers is broken. By using a smoothing method, such an unnatural channel fluctuation of data-aided CSI can be mitigated by refining the frequency selectivity. The following subsections introduce the representative smoothing methods and derive the suitable one for our proposed approach concretely.

A. SMOOTHING METHOD

Smoothing methods can compensate discrete or scattered outliers and estimate smoother transition than the original information. These techniques are applied as preprocessing in order to correct data originally having continuity or mutuality. These preprocessing for data sets are especially important to conduct machine training accurately. The well-known smoothing methods are the moving average (MA) and Savitzky-Golay (SG) filtering. Each smoothing method has respective features of calculating a smoothing value, and there is a possibility that the optimal smoothing scheme is different depending on the problem and target. On that account, the SG filter is suitable for the proposed approach. It is elaborated by the simulation results of performance comparison in Section V.

1) MOVING AVERAGE (MA)

The simplest method for data smoothing is symmetrical MA, whose smoothed value at the i-th explanatory variable, $\hat{u}(i)$, is defined as follows.

$$\hat{u}(i) = \frac{\sum_{j=i-M}^{i+M} u(j)}{2M+1}, \tag{14}$$

where M denotes the unilateral window size; the whole window size applied for smoothing is $2M + 1$. $u(j)$ represents the original value at the j-th explanatory variable. In this method, all values in a smoothing window are equivalent to averaging. Thus, there are some cases that values at the edge of a smoothing window are too much influenced for a smoothed value. There are linearly weighted moving average (LWMA) and exponentially weighted moving average (EWMA) that add weights to raw data with how close the object position is in mind. The smoothed values of these methods are obtained by

$$\hat{u}(i) = \frac{\sum_{j=i-M}^{i+M} \{(M - |i-j| + 1)u(j)\}}{\sum_{j=i-M}^{i+M} (M - |i-j| + 1)}, \tag{15}$$

$$\hat{u}(i) = \frac{\cdots + \alpha u(i-1) + u(i) + \alpha u(i+1) + \cdots}{\cdots + \alpha + 1 + \alpha + \cdots}. \tag{16}$$

Here, α $(0 < \alpha < 1)$ denotes a constant smoothing factor. In EWMA, the weights fluctuation does not reach anywhere zero. The whole raw data is concerned for the calculation of smoothing value using (16). As shown in (15) and (16), the former diminishes a weight value linearly; in contrast, a weight value of the latter is lessened non-linearly. Therefore, LWMA is suitable for weighted average with restricting smoothing window, and EWMA can make much account of adjusting values and cannot abandon distant data.

2) SAVITZKY-GOLAY (SG) FILTERING

The Savitzky-Golay (SG) filtering was initially proposed in 1964 [30]. Even now, the SG filter is mainly used for noisy data in spectral analysis, and various improvements of the SG filter have been studied. Also, it was shown that the SG filter is adequate for smoothing time-series data in the literature [31]–[33]. SG filtering conducts an arbitrary order polynomial approximation using the least square method in an object of a window section. A smoothed value obtained by the SG method is defined as an output value of the approximated polynomial at the center of the window section. We give the precise method of calculation to extract the smoothed value at the i-th explanatory variable, which is assumed to be p below.

Fig. 6 exhibits the overview of smoothing-based SG filtering. At first, we perform coordinate transformation for p to generalize the explanation of this problem. The transformed explanatory variable, q, is defined as,

$$q = p - i. \tag{17}$$

This transformation moves the position from i to 0 in parallel. Accordingly, $q = 0$ and $p = i$ are the same positions in the

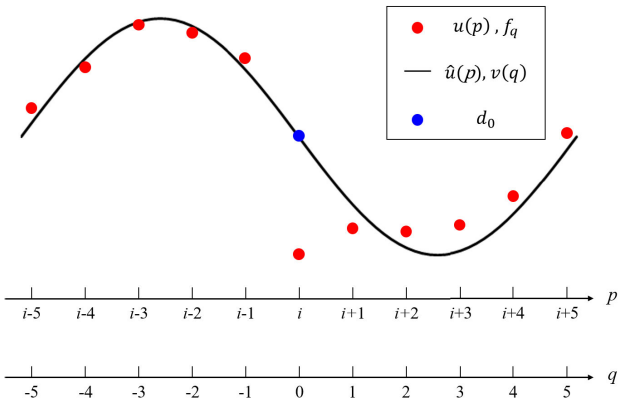

FIGURE 6. Overview of smoothing based on SG filter.

explanatory variable direction. Based on this transformation, we describe how to obtain the smoothed value of the SG filter at $q = 0$ from this point. First, the N-th degree function of q, $v(q)$, in the transformed window area is defined as,

$$v(q) = \sum_{n=0}^{N} q^n d_n, \tag{18}$$

where d_n is the regression coefficient of the n-th degree of q. The definition vector of regression coefficients is,

$$\mathbf{d} = \begin{bmatrix} d_0 & d_1 & d_2 & \cdots & d_N \end{bmatrix}^{\mathsf{T}}. \tag{19}$$

The vectors of explanatory variables and objective variables are defined as

$$\mathbf{Q} = \begin{bmatrix} 1 & -M_{SG} & (-M_{SG})^2 & \cdots & (-M_{SG})^N \\ \vdots & \vdots & \vdots & \cdots & \vdots \\ 1 & -1 & (-1)^2 & \cdots & (-1)^N \\ 1 & 0 & 0 & \cdots & 0 \\ 1 & 1 & 1^2 & \cdots & 1^N \\ \vdots & \vdots & \vdots & \cdots & \vdots \\ 1 & M_{SG} & M_{SG}^2 & \cdots & M_{SG}^N \end{bmatrix}, \tag{20}$$

$$\mathbf{f} = \begin{bmatrix} f_{-N} & \cdots & f_{-1} & f_0 & f_1 & \cdots & f_N \end{bmatrix}^{\mathsf{T}}, \tag{21}$$

where f_q presents the objective value, i.e. CSI at the q-th subcarrier obtained by PCE and DFCE in the proposed method. This is the same as $u(p - i)$. The normal equation of least square method is given by,

$$\mathbf{Q}^{\mathsf{T}}\mathbf{f} = \mathbf{Q}^{\mathsf{T}}\mathbf{Q}\mathbf{d}. \tag{22}$$

By variation of Eq. (22), we can obtain the values of $\mathbf{d}$ using the following equation:

$$\mathbf{d} = (\mathbf{Q}^{\mathsf{T}}\mathbf{Q})^{-1}\mathbf{Q}^{\mathsf{T}}\mathbf{f} = \mathbf{Z}\mathbf{f}, \tag{23}$$

where $\mathbf{Z} = (\mathbf{Q}^{\mathsf{T}}\mathbf{Q})^{-1}\mathbf{Q}^{\mathsf{T}}$. Thus, the regression coefficients are obtained and the SG filter can express the approximate equation of arbitrary order. From (17), the smoothed value at $p = i$ is represented as the polynomial approximation of the SG filtering result at $q = 0$. The constant term, d_0, is only remained when 0 is substituted for q in Eq. (18). Accordingly, the smoothed value at $p = i$ is expressed as,

$$\begin{aligned} \hat{u}(i) &= v(0) = d_0 \\ &= Z(1,1)f_{-N} + Z(1,2)f_{-N+1} + \cdots \\ &\quad + Z(1, M_{SG} - 1)f_{N-1} + Z(1, M_{SG})f_N, \end{aligned} \tag{24}$$

where $Z(a, b)$ denotes the matrix element of $\mathbf{Z}$ at the a-th row ($1 \le a \le N + 1$) and b-th column ($1 \le b \le 2M_{SG} + 1$). $\mathbf{Z}$ can usually be calculated in advance by defined the number of N and M_{SG}. For that reason, SG filtering is practically conducted with (21) and (24) only. This smoothed scheme is basically applied for all data areas in an explanatory variable (but except for circumferential parts of both ends). Incidentally, transitions of obtained expressions in $p = M_{SG} + 1$ and $p = L_d - M_{SG}$ is applied in $1 \le p \le M_{SG}$ and $L_d - M_{SG} + 1 \le p \le L_d$ using (18) and (23). Here, L_d denotes the all length of data area processed smoothing. We can eventually obtain a smoothed transition of all data and remove the influence of noisy or scattered information by these processes.

B. INCORPORATION WITH GRNN TRAINING AND CHANNEL TRACKING

The proposed scheme employs the smoothing approach in the frequency-domain after the DFCE process. In this method, the SG filtering process is inserted between the DFCE block and desired responses block of Fig. 5. It can compensate for the influence of inaccurate CSI before GRNN training. Due to the preprocessing of desired symbols, GRNN estimates whole channel state transitions more precisely than the conventional approach.

Fig. 7 shows the process of the proposed scheme. Using the pilot symbol, the first symbol's CSI is estimated by PCE in (12), and the 10th symobol's CSI estimated by DFCE in (8) is treated as the training input data for GRNN. After CSI estimation, the smoothing method is applied to DFCE-based CSIs in the frequency domain. SG filtering enables to optimize the value of CSI, which improves the channel compensation performance by GRNN. Here, the channel $\tilde{H}$ for $p = i$ smoothed by the SG filtering is represented as follows,

$$\hat{h}_{smooth}(p) = Z(1,1)\hat{H}(-N) + \cdots + Z(1, M_{SG})\hat{H}(N), \tag{25}$$

On the other hand, for $1 \le p \le M_{SG}$ and $(L_d - M_{SG} + 1) \le p \le L_d$,

$$\hat{\mathbf{h}}_{smooth} = \mathbf{Z}\hat{\mathbf{H}} \sum_{n=0}^{N} (p - i)^n, \tag{26}$$

This smoothing can remove inaccurate frequency responses, e.g. outliers, without degradation of frequency selectivity and obtain the refined CSI, $\hat{\mathbf{h}}_{smooth} = (\hat{h}_{smooth}(1), \hat{h}_{smooth}(2), \ldots, \hat{h}_{smooth}(N_c))$. Then PCE-based CSIs and smoothed DFCE-based CSIs are set as the desired symbols. Symbol indices (1, 10) are defined as the

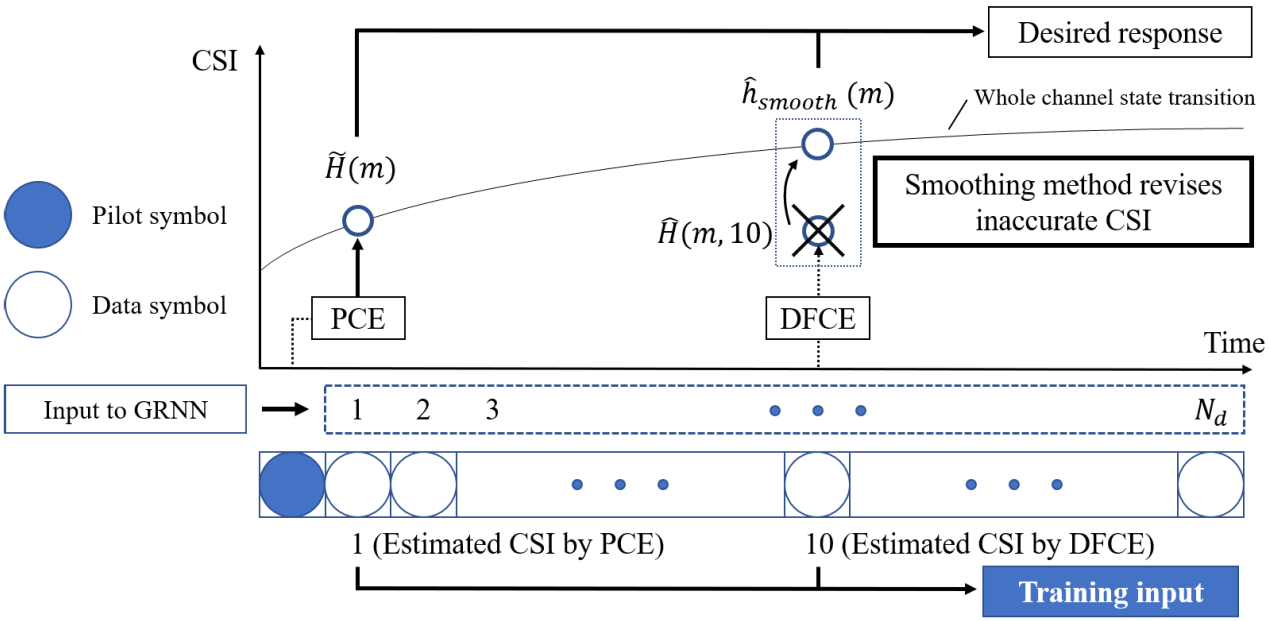

FIGURE 7. Concept of the proposed method.

TABLE 1. Simulation parameters.

Transmission scheme	OFDM
Data modulation	QPSK
FFT size, Number of carriers	64
Guard interval	16
Number of pilot/data symbols	$N_p = 1, N_d = 20$
Channel model	15 path Rayleigh fading
Path interval	1
Max Doppler frequency	700 Hz
Transmission bandwidth	20 MHz
Forward error correction	Convolutional code ($R = 1/2, K = 7$)
Radius of RBF	$r = 4.5$

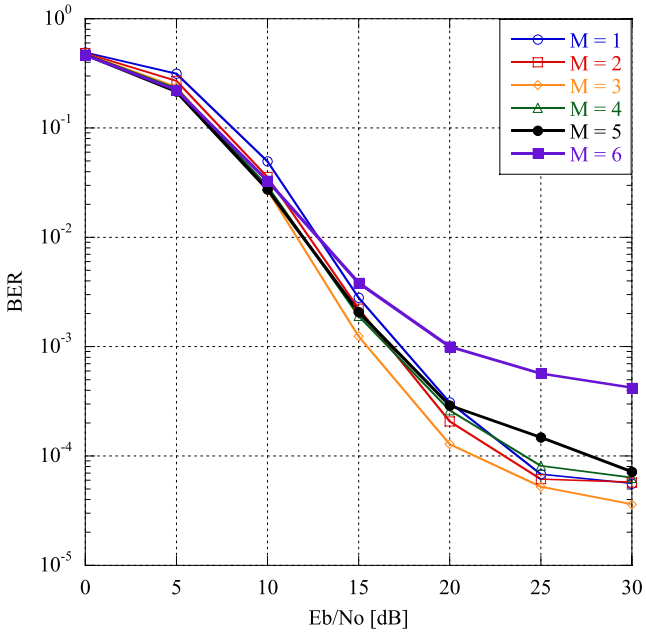

FIGURE 8. BER performance of various unilateral window size *M* for the proposed method using MA.

training inputs. Lastly, same as the conventional scheme, the index vector for all data symbols is entered into the GRNN. Thanks to improved accuracy of the desired responses, GRNN can produce $\mathbf{H}_{out}$ more accurately, and this information can be utilized for channel tracking.

V. COMPUTER SIMULATION

A. SIMULATION RESULTS

The simulation parameters are shown in Table 1, here N_p denotes the number of pilot symbols. The maximum Doppler frequency is set as 700 Hz to represent a fast fading environment, and its normalized value is 2.8×10^{-3} per OFDM symbol duration. Radius of RBF r is 4.5 in the proposed method.

At first, the best parameters for each smoothing method are examined by comparing the bit error rate (BER) value of the CSI estimate in this simulation condition. Fig. 8 shows the BER performance of various unilateral window size M for

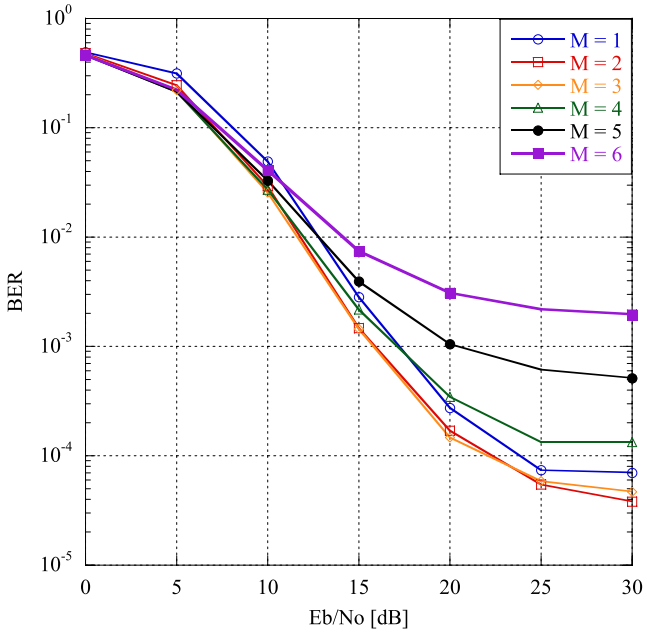

FIGURE 9. BER performance of various unilateral window size M for the proposed method using LWMA.

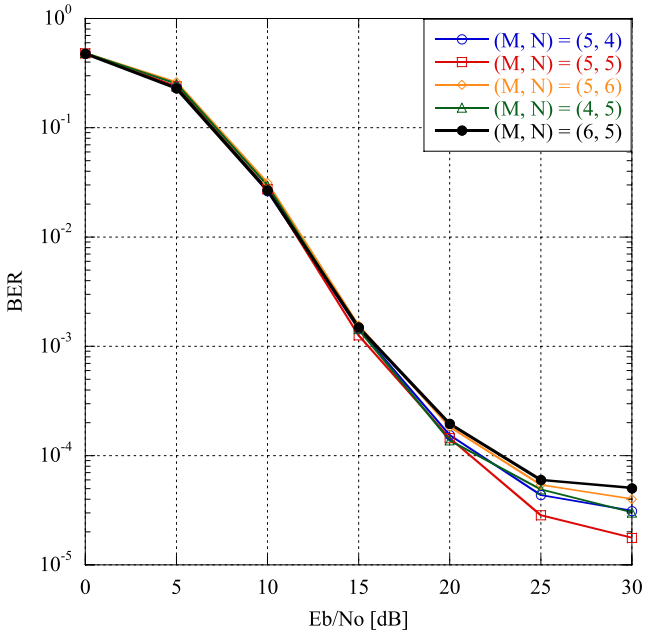

FIGURE 11. BER performance of maximum degree N and unilateral window size M for the proposed method using SG.

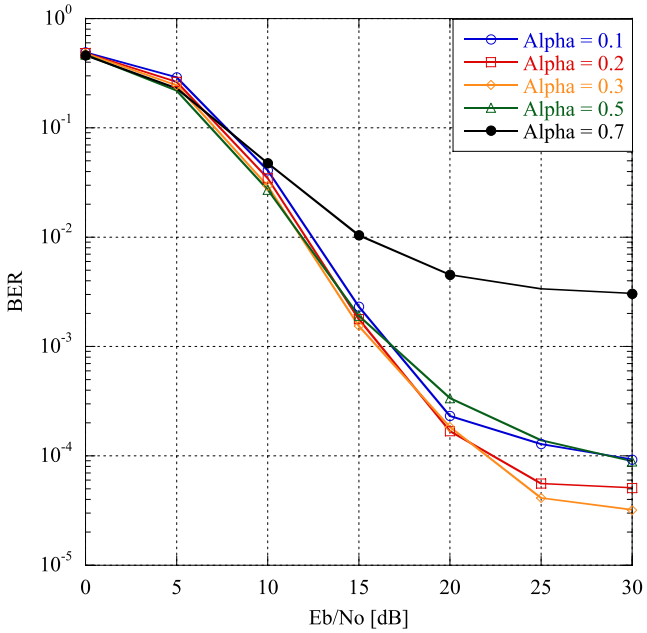

FIGURE 10. BER performance of various constant smoothing factor α for the proposed method using EWMA.

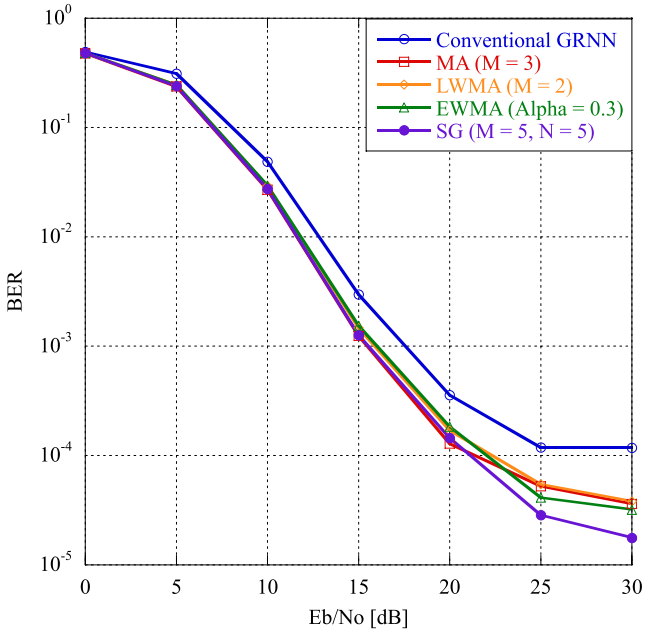

FIGURE 12. Performance comparison of smoothing methods.

the revised method when MA is introduced in the smoothing process. The best BER performance is shown for $M = 3$. The optimal window size M could depend on the coherence bandwidth. This parameter setting is based on Wi-Fi systems with relatively wider subcarrier spacing than cellular-based specifications such as LTE or WiMAX. It also implies that the MA-based approaches do not apply to the channel environment having dynamic frequency selectivity.

Fig. 9 shows the BER performance which adopts LWMA. In smoothing with LWMA, the best BER performance is observed when M is 2 and 3. compared to MA, the range of performance degradation due to M is wide. From (15), since LWMA performs smoothing with a larger amount of information than MA when M becomes too large, even harmful effects are captured and smoothed, resulting in significant degradation of BER.

Fig. 10 presents the BER performance of the various smoothing factor α for the proposed method when EWMA is introduced in the smoothing process. As shown from this graph, setting α to 0.3 achieves the best BER performance.

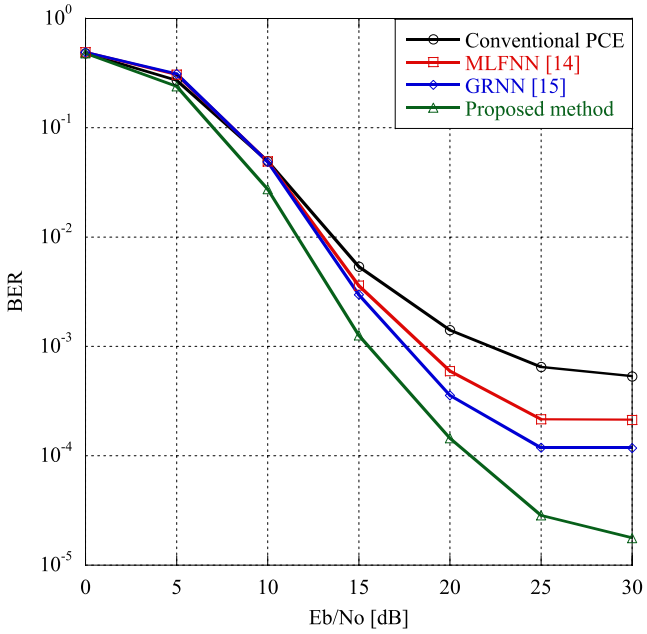

FIGURE 13. BER performance compared to various conventional methods.

When α is 0.7, the BER performance is the most degraded. In EWMA, as α increases, the influence of distant data becomes stronger, resulting in significant performance degradation.

Fig. 11 plots the BER performance of the maximum degree of approximation function N and M (after coordinate transformation) for the revised method when SG filtering is applied in the smoothing process. When both N and M are 5, the best BER performance can be attained. From these preliminary parameter comparisons, we apply parameters as $M = 3$ for MA, $M = 2$ for LWMA, $\alpha = 0.3$ for EWMA, and $M = 5$ and $N = 5$ for the SG filtering.

Smoothing methods are then compared using the above parameters. Fig. 12 shows the comparison results of the smoothing methods. Each smoothing method is employed after DFCE part. All channel tracking performance using smoothing method can be improved in both metrics against the conventional GRNN approach. MA and LWMA should always contain adjacent data values, and it may limit the effectiveness of CSI smoothing in a wide subcarrier spacing setting. Meanwhile, the SG filtering based scheme exhibit the lowest BER value. From this result, SG filtering is introduced for the smoothing part of the proposed method hereafter.

Fig. 13 presents the BER performances of the conventional PCE, MLFNN [14], GRNN-based method [15], and the proposed method that employs SG filtering. The BER performance of the PCE is seriously deteriorated because decision errors are frequently happened in the last part of the packet; it shows an error floor. MLFNN-based method shows superior performance compared to the conventional PCE, but the BER never reaches 10^{-4} and an error floor occurs. This is due to the fact that the generalization capability by MLFNN is not able to track the channel tracking sufficiently. The conventional GRNN-based method presents the better BER performance than the PCE and MLFNN methods, however, the error floor still remains around 10^{-4}. On the other hand, the proposed method shows the best BER performance, achieving a value close to 10^{-5}. It can be confirmed that the proposed method obtains excellent performance even in a fast-moving environment because the smoothing on the CSI, which is the supervised data, can make full use of the superior generalization capability of GRNN. Based on this result, the proposed method can compensate for inaccurate CSI estimates derived from DFCE and improved channel tracking performance by fully leveraging GRNN capability for all data symbols. From these results, our proposed GRNN-based channel tracking with the smoothing filter is quite effective to realize stable wireless communication in a high mobility environment.

TABLE 2. Time cost by various methods.

	Processing time [ms]	BER
MLFNN [15]	90.3102	2.1×10^{-4}
GRNN [16]	0.0534	1.2×10^{-4}
MA (M = 3)	0.0094	–
LWMA (M = 2)	0.1034	–
EWMA (α = 0.3)	0.1474	–
SG (M = 5, N = 5)	0.3519	–
Proposal	0.4206	1.8×10^{-5}

B. COMPUTATION COMPLEXITY

This section compares MLFNN [14], GRNN-based method [15], and the proposed method in terms of computation complexity. All methods use DFCE for channel estimation, therefore, its complexity is not considered. At first, the computation complexity of MLFNN can be expressed as follows,

$$\Upsilon_{MLFNN} = N_{hidden}(N_{input} + N_{output}), \tag{27}$$

where N_{input} is the number of the network input, N_{hidden} is the number of hidden layers, and N_{output} is the number of outputs. Similarly, for GRNN, it can be represented as,

$$\Upsilon_{GRNN} = N_{hidden}(N_{input} + N_{output} + 1) + N_{output}. \tag{28}$$

In the proposed method, smoothing by SG is performed on the estimated CSI. Its computation complexity is expressed as follows,

$$\begin{aligned}\Upsilon_{SG} = {} & (2M_{SG} + 1)(Ld - (2M_{SG} + 1) \\ & + 2(N + 1)(2M_{SG} + 1 + N).\end{aligned} \tag{29}$$

Table 2 summarizes the CPU processing time consumed for channel estimation and BER at SNR = 30 dB of each method. For the computation environment, Intel(R)

Core(TM) i9-10900K CPU @ 3.70 GHz and 64 GB memory are used. Here, the processing time is measured and averaged over 10000 trials. As can be seen from the table, the processing speed of GRNN is much faster than that of MLFNN. MLFNN requires only a small amount of computation to implement once training is completed, but the running time required for convergence is enormous. On the other hand, because the computational cost for training GRNN is minimal, it shows a high processing time for solving problems that require online phase processing, such as those considered in the proposed method. Since the computation cost of the SG smoothing is heavy, it increases overall processing time for the proposed method. Meanwhile, its BER performance can be improved significantly; such additional processing can be allowable considering practical hardware implementation.

VI. DISCUSSION

The most significant factor affecting the channel tracking and compensation is the Doppler shift caused by the moving velocity. The proposed method performs accurate channel tracking from a small number of CSI data and is completed only in the online phase. Hence, the proposed method can achieve robust channel tracking to changes in moving speed. In this paper, we have shown the effectiveness of the proposed method by using only simulated data. The proposed method is expected to be still effective even when using actual data, when CSI as the supervised data can be estimated correctly to a certain extent. It should be further investigated as our future work.

VII. CONCLUSION

In this paper, we proposed the GRNN based channel tracking method that applied the smoothing preprocessing in order to refine incorrect desired responses produced by DFCE. From the comparison of smoothing candidates, SG filtering is the most effective for refining inaccurate CSI outliers without disruption of original channel frequency selectivity. It can reduce the impact of erroneous CSI estimation by DFCE and improve the whole channel tracking capability of GRNN. Therefore the proposed method has provided the best BER performance compared with the conventional PCE and our previous GRNN-based method even at a maximum Doppler frequency of 700 Hz. Accordingly, we can conclude that the proposed approach can be the most suitable channel tracking method even in high mobility communication environment.

REFERENCES

[1] F. Adachi, "BER analysis of 2PSK, 4PSK, and 16QAM with decision feedback channel estimation in frequency-selective slow Rayleigh fading," *IEEE Trans. Veh. Technol.*, vol. 48, no. 5, pp. 1563–1572, Sep. 1999.

[2] B. Yang, Z. Cao, and K. B. Letaief, "Analysis of low-complexity windowed DFT-based MMSE channel estimator for OFDM systems," *IEEE Trans. Commun.*, vol. 49, no. 11, pp. 1977–1987, Nov. 2001.

[3] H. Minn, D. I. Kim, and V. K. Bhargava, "A reduced complexity channel estimation for OFDM systems with transmit diversity in mobile wireless channels," *IEEE Trans. Commun.*, vol. 50, no. 5, pp. 799–807, May 2002.

[4] W.-G. Song and J.-T. Lim, "Pilot-symbol aided channel estimation for OFDM with fast fading channels," *IEEE Trans. Broadcast.*, vol. 49, no. 4, pp. 398–402, Dec. 2003.

[5] O. Simeone, Y. Bar-Ness, and U. Spagnolini, "Pilot-based channel estimation for OFDM systems by tracking the delay-subspace," *IEEE Trans. Wireless Commun.*, vol. 3, no. 1, pp. 315–325, Jan. 2004.

[6] F. N. Khan, K. Zhong, W. H. Al-Arashi, C. Yu, C. Lu, and A. P. T. Lau, "Modulation format identification in coherent receivers using deep machine learning," *IEEE Photon. Technol. Lett.*, vol. 28, no. 17, pp. 1886–1889, Sep. 1, 2016.

[7] Y. Wang, M. Liu, J. Yang, and G. Gui, "Data-driven deep learning for automatic modulation recognition in cognitive radios," *IEEE Trans. Veh. Technol.*, vol. 68, no. 4, pp. 4074–4077, Apr. 2019.

[8] S. Kojima, K. Maruta, and C.-J. Ahn, "Adaptive modulation and coding using neural network based SNR estimation," *IEEE Access*, vol. 7, pp. 183545–183553, 2019.

[9] M. Alymani, M. H. Alhazmi, A. Almarhabi, H. Alhazmi, A. Samarkandi, and Y.-D. Yao, "Rician K-factor estimation using deep learning," in *Proc. 29th Wireless Opt. Commun. Conf. (WOCC)*, May 2020, pp. 1–4.

[10] S. Kojima, K. Maruta, Y. Feng, C.-J. Ahn, and V. Tarokh, "CNN-based joint SNR and Doppler shift classification using spectrogram images for adaptive modulation and coding," *IEEE Trans. Commun.*, vol. 69, no. 8, pp. 5152–5167, Aug. 2021.

[11] M. Sánchez-Fernández, M. de Prado-Cumplido, J. Arenas-García, and F. Pérez-Cruz, "SVM multiregression for nonlinear channel estimation in multiple-input multiple-output systems," *IEEE Trans. Signal Process.*, vol. 52, no. 8, pp. 2298–2307, Aug. 2004.

[12] H. Ye, G. Y. Li, and B.-H. Juang, "Power of deep learning for channel estimation and signal detection in OFDM systems," *IEEE Wireless Commun. Lett.*, vol. 7, no. 1, pp. 114–117, Feb. 2018.

[13] H. Huang, J. Yang, H. Huang, Y. Song, and G. Gui, "Deep learning for super-resolution channel estimation and DOA estimation based massive MIMO system," *IEEE Trans. Veh. Technol.*, vol. 67, no. 9, pp. 8549–8560, Sep. 2018.

[14] T. Omura, S. Kojima, K. Maruta, and C.-J. Ahn, "Neural network based channel identification and compensation," *IEICE Commun. Exp.*, vol. 8, no. 10, pp. 416–421, 2019.

[15] T. Omura, N. Hoeur, K. Maruta, and C.-J. Ahn, "Improving ANN based channel identification and compensation using GRNN method under fast fading environment," in *Proc. Int. Conf. Adv. Technol. Commun. (ATC)*, Oct. 2019, pp. 28–32.

[16] A. Goldsmith, *Wireless Communications*. Cambridge, U.K.: Cambridge Univ. Press, Aug. 2005.

[17] J. Proakis, *Digital Communications*. New York, NY, USA: McGraw-Hill, Nov. 2007.

[18] T. Rappaport, R. Heath, Jr., R. Daniels, and J. Murdock, *Millimeter Wave Wireless Communications*. Upper Saddle River, NJ, USA: Prentice-Hall, Sep. 2014.

[19] R. H. Clarke, "A statistical theory of mobile radio reception," *Bell Syst. Tech. J.*, vol. 47, no. 6, pp. 957–1000, 1968.

[20] Y. Ida, M. Yofune, C.-J. Ahn, T. Matsumoto, and S. Matsufuji, "Estimation based on weighted channel variance for HTRCI-MIMO/OFDM with QRM-MLD and channel ranking under fast fading channel," *Trans. Emerg. Telecommun. Technol.*, vol. 26, no. 7, pp. 1050–1059, Jul. 2015.

[21] M. Yofune, C. Ahn, T. Kamio, H. Fujisaka, and K. Haeiwa, "Decision direct and linear prediction based fast fading compensation for TFIOFDM," *Far East J. Electron. Commun.*, vol. 3, no. 1, pp. 35–52, Jul. 2007.

[22] S. Soejima, Y. Ida, C.-J. Ahn, T. Omori, and K.-Y. Hashimoto, "Fast fading compensation based on weighted channel variance for TFI-OFDM," *J. Signal Process.*, vol. 17, no. 3, pp. 41–49, 2013.

[23] Z. Ghassemlooy, W. Popoola, and S. Rajbhandari, *Optical Wireless Communications: System and Channel Modelling With MATLAB*. Boca Raton, FL, USA: CRC Press, Mar. 2017.

[24] K. Burse, R. N. Yadav, and S. C. Shrivastava, "Channel equalization using neural networks: A review," *IEEE Trans. Syst., Man, Cybern. C, Appl. Rev.*, vol. 40, no. 3, pp. 352–357, May 2010.

[25] S. Haykin, *Neural Networks: A Comprehensive Foundation*, 2nd ed. Upper Saddle River, NJ, USA: Prentice-Hall, Jul. 1998.

[26] D. F. Specht, "A general regression neural network," *IEEE Trans. Neural Netw.*, vol. 2, no. 6, pp. 568–576, Nov. 1991.

[27] M. Nama and A. Shaker, "Function approximation using neural and fuzzy methods," *Commun. Appl. Electron.*, vol. 6, no. 3, pp. 35–42, Nov. 2016.

[28] S. Yang, T. O. Ting, K. L. Man, and S. U. Guan, "Investigation of neural networks for function approximation," *Proc. Comput. Sci.*, vol. 17, pp. 586–594, Oct. 2013.
[29] F. Heimes and B. Heuvein, "The normalized radial basis function neural network," in *Proc. IEEE Int. Conf. Syst., Man, Cybern.*, vol. 2, Nov. 1998, pp. 1609–1614.
[30] A. Savitzky and M. J. E. Golay, "Smoothing and differentiation of data by simplified least squares procedures," *Anal. Chem.*, vol. 36, no. 8, pp. 1627–1639, 1964.
[31] S. V. Menon and C. S. Seelamantula, "Robust Savitzky–Golay filters," in *Proc. 19th Int. Conf. Digit. Signal Process.*, Aug. 2014, pp. 688–693.
[32] H. Kaneko and K. Funatsu, "Smoothing-combined soft sensors for noise reduction and improvement of predictive ability," *Ind. Eng. Chem. Res.*, vol. 54, no. 50, pp. 12630–12638, Dec. 2015.
[33] H. Kaneko and K. Funatsu, "Improvement of process state recognition performance by noise reduction with smoothing methods," *J. Chem. Eng. Jpn.*, vol. 50, no. 6, pp. 422–429, 2017.

SHUN KOJIMA (Member, IEEE) received the B.E., M.E., and Ph.D. degrees in electrical and electronics engineering from Chiba University, Japan, in 2017, 2018, and 2021, respectively. He is currently an Assistant Professor at the Graduate School of Engineering, Utsunomiya University. His research interests include machine learning, wireless communications, and signal processing. He is a member of IEICE. He received the SoftCOM Best Paper Award, in 2018, the 3rd Communication Quality Student Workshop Best Poster Award, in 2019, the IEEE VTS Tokyo/Japan Chapter 2020 Young Researcher's Encouragement Award, in 2020, the RISP Best Paper Award, in 2021, and the IEICE Radio Communication Systems Active Researcher Award, in 2021.

HE HE (Graduate Student Member, IEEE) received the B.E. degree in electrical and electronics engineering from Dalian Maritime University, Dalian, China, in 2018, and the M.E. degree in electrical and electronics engineering from Chiba University, Chiba, Japan, in 2020, where he is currently pursuing the Ph.D. degree. His research interests include machine learning and the development of next-generation communication algorithm.

TAKAKI OMURA received the B.E. and M.E. degrees from Chiba University, Japan, in 2018 and 2020, respectively. He is currently a Staff Member of SoftBank Corporation. His research interests include OFDM and channel estimation using RBF networks for wireless communication in high mobility environment.

KAZUKI MARUTA (Senior Member, IEEE) received the B.E., M.E., and Ph.D. degrees in engineering from Kyushu University, Japan, in 2006, 2008, and 2016, respectively. From 2008 to 2017, he was with NTT Access Network Service Systems Laboratories and was engaged in the research and development of interference compensation techniques for future wireless communication systems. From 2017 to 2020, he was an Assistant Professor with the Graduate School of Engineering, Chiba University. He is currently a Specially Appointed Associate Professor with the Academy for Super Smart Society, Tokyo Institute of Technology. His research interests include MIMO, adaptive array signal processing, channel estimation, medium access control protocols, and moving networks. He is a Senior Member of IEICE. He received the IEICE Young Researcher's Award, in 2012, the IEICE Radio Communication Systems (RCS) Active Researcher Award, in 2014, the Asia–Pacific Microwave Conference (APMC) Prize, in 2014, and the IEICE RCS Outstanding Researcher Award, in 2018. He was a co-recipient of the IEICE Best Paper Award, in 2018.

CHANG-JUN AHN (Senior Member, IEEE) received the Ph.D. degree from the Department of Information and Computer Science, Keio University, Japan, in 2003. From 2001 to 2003, he was a Research Associate with the Department of Information and Computer Science, Keio University. From 2003 to 2006, he was with the Communication Research Laboratory, Independent Administrative Institution (now the National Institute of Information and Communications Technology). In 2006, he was on assignment at ATR Wave Engineering Laboratories. In 2007, he was with the Faculty of Information Sciences, Hiroshima City University, as a Lecturer. He is currently working at the Graduate School of Engineering, Chiba University, as a Professor. His research interests include OFDM, digital communication, channel coding, and signal processing for telecommunications. He is a Senior Member of IEICE. From 2005 to 2006, he was an Expert Committee Member of Emergence Communication Committee, Shikoku Bureau of Telecommunications, and Ministry of Internal Affairs and Communications (MIC), Japan. He received the ICF Research Grant Award for Young Engineer, in 2002, the Funai Information Science Award for Young Scientist, in 2003, the Distinguished Service Award from Hiroshima City, in 2010, the IEEE SoftCOM2018 Best Paper Award, in 2018, the IEEE APCC2019 Best Paper Award, in 2019, the IEICE ICETC2020 Best Paper Award, in 2020, and the Journal of Signal Processing Best Paper Award, in 2021. He served as an Associate Editor for the *IEICE Transactions on Fundamentals of Electronics, Communications and Computer Sciences*.